Regional ventilation distribution and respiratory mechanical assessment of pressure-regulated volume control versus volume-control ventilation in healthy and injured rabbit lung

Journal:	*British Journal of Anaesthesia*
Manuscript ID:	Draft
Manuscript Type:	Laboratory Investigation
Date Submitted by the Author:	n/a
Complete List of Authors:	Porra, Liisa; University of Helsinki, Departmenet of Physics Bayat, Sam; Université de Picardie Jules Verne - Médecine, Physiologie; CHU Amiens, Cardiologie et Pneumologie Pédiatriques Malaspinas, Iliona; University of Geneva, Anaesthesiological Investigational Unit Albu, Gergely; University of Geneva, Anaesthesiological Investigational Unit Doras, Camille; University of Geneva, Anaesthesiological Investigational Unit Broche, Ludovic; European Synchrotron Radiation Facility, Biomedical Beamline-ID17 Strengell, Satu; University of Helsinki, Departmenet of Physics Petak, Ferenc; University of Szeged, Department of Medical Physics and Informatics Habre, Walid; Geneva Children's Hospital, Paediatric Anaesthesia Unit
Key Words:	Ventilation - mechanical, MONITORING - respiratory, GAS EXCHANGE, Lung - damage, RESPIRATORY - mechanics

REGIONAL VENTILATION DISTRIBUTION AND RESPIRATORY MECHANICAL ASSESSMENT OF PRESSURE-REGULATED VOLUME CONTROL VERSUS VOLUME-CONTROL VENTILATION IN HEALTHY AND INJURED RABBIT LUNG

[1]Liisa Porra, [2]Sam Bayat, [3]Iliona Malaspinas, [3]Gergely Albu, [3]Camille Doras, [2,4]Ludovic Broche, [1]Satu Strengell, [5]Ferenc Peták, [6]Walid Habre

Institutions:

[1] Department of Physics, University of Helsinki, Helsinki, Finland

[2] Université de Picardie Jules Verne, Inserm U1105 and Paediatric Lung Function Laboratory, CHU Amiens, Amiens, France

[3] Anesthesiological Investigation Unit, University of Geneva, Geneva, Switzerland

[4] European Synchrotron Radiation Facility, Biomedical Beamline-ID17, Grenoble, France

[5] Department of Medical Physics and Informatics, University of Szeged, Szeged, Hungary

[6] Geneva Children's Hospital, University Hospitals of Geneva and Geneva University, Geneva, Switzerland

Corresponding Author: Walid Habre
Paediatric Anaesthesia Unit
Geneva Children's Hospital
6, Rue Willy Donzé, CH-1205 Geneva, Switzerland
Tel: +41-22-3827504
Fax: +41-22-3825485
Email: walid.habre@hcuge.ch

Short running title: Ventilation mode and regional lung function

Word count: Abstract: 250; Introduction: 438; Discussion: 1009.

ABSTRACT

Background: It is not well known how ventilation modes might affect the regional distribution of ventilation within the lung. In this study, we compared respiratory mechanics, lung aeration and regional specific ventilation ($s\dot{V}$) distributions in healthy and surfactant-depleted rabbits ventilated with pressure regulated volume control mode (PRVC) with a decelerating inspiratory flow, or volume control (VC).

Methods: New-Zealand White rabbits (n=8) were anaesthetized, paralyzed and mechanically ventilated either with VC (Vt: 7ml/kg; RR: 30/min; PEEP: 3 cmH_2O) or PRVC (target VT: 7 ml/kg), at baseline and after lung injury induced by lung lavage (LL). Airway resistance (Raw), respiratory tissue damping (G) and elastance (H) were measured by low-frequency forced oscillations. Synchrotron radiation computed tomography during stable xenon washin was used to measure regional lung aeration and specific ventilation and the relative fraction of atelectatic, air-trapping, normally-, poorly- and hyper-inflated lung regions.

Results: Lung lavage significantly elevated both driving ($P_{driving}$) and peak (P_{peak}) pressures ($p<0.001$), while both of these parameters remained lower on PRVC (-14.0±1.7%, $p<0.001$; -12.7±1.7%, $p<0.001$ for $P_{driving}$ and P_{peak}, respectively). No significant differences in respiratory mechanics, regional ventilation distribution or blood oxygenation could be detected between the 2 ventilation modes.

Conclusions: The assessment of two common mechanical ventilation modes revealed the advantage of applying a decelerating flow (PRVC) to achieve equivalent regional and global lung function in both normal and mechanically heterogeneous lungs, since both $P_{driving}$ and P_{peak} were significantly lower, suggesting reduced mechanical stresses under this ventilation mode.

Keywords: Lung injury; Synchrotrons; Respiratory Mechanics; Respiration, Artificial; Xenon; Tomography, X-Ray Computed.

INTRODUCTION

Mechanical ventilation is an essential supportive measure, which allows maintaining alveolar ventilation and blood oxygenation both in routine anaesthesia and in the care of the critically ill patient. However, mechanical stresses during positive pressure ventilation may also have deleterious pulmonary consequences, leading to inflammation, adverse structural and functional changes as well as compromised haemodynamics due to impeded venous return[1]. These factors can significantly contribute to respiratory morbidity and mortality in mechanically-ventilated patients. Optimizing tidal volume and driving pressures during mechanical ventilation in order to obtain the best possible gas exchange with minimal mechanical stresses to the lung remains a major challenge. Traditional ventilator modes allow setting a desired tidal volume or peak inspiratory pressure. Modern mechanical ventilators provide more sophisticated ventilation modes such as pressure-regulated volume-control (PRVC), an assist/control mode of ventilation. In this mode, the delivery of tidal volume is guaranteed without exceeding a pre-set inspiratory pressure limit, by decelerating inspiratory flow and modifying inspiratory time, on a cycle to cycle basis.

Previous studies have assessed the differences between PRVC and conventional volume-control ventilation (VC) in both infants and adults[2-4]. These studies suggest that PRVC allows reducing peak inspiratory pressures, while maintaining similar cardiac output, airway pressures, and gas exchange[4]. Exaggerated local mechanical stresses are primarily responsible for injuring the lung tissue[5], and these forces are directly determined by the transpulmonary pressure. This implies that maintaining a similar ventilator goal with a lower inspiratory pressure should have beneficial effects.

Currently, it is not well known how ventilation modes might alter the regional distribution of ventilation within the lung. To our knowledge, the few experimental and clinical studies of the differences in lung function between different ventilation modes have not addressed the question of regional functional and structural differences within the lung[3, 6]. We have developed a xenon-enhanced computed tomography technique that uses synchrotron-generated x-rays to simultaneously image lung morphology and tissue density, as well as the regional distribution of ventilation[7, 8]. We have previously shown that combining data on regional lung aeration and regional ventilation allows defining a spectrum of regional mechanical behaviours ranging from tidal recruitment to complete air trapping[7]. Application of this functional imaging technique in combination with the assessment of airway and respiratory tissue mechanics allows a detailed assessment of the conducting airways and alveolar compartments under different ventilation modes.

The goal of the present study was therefore to compare the effects of PRVC and VC on the distribution of regional lung aeration and ventilation using synchrotron radiation imaging. We also assessed the forced oscillatory mechanics of the respiratory system with both ventilation modes in normal lung and after inducing lung injury by surfactant depletion in anesthetized rabbits.

MATERIALS AND METHODS

Animal preparation

The procedures for the animal care and the experiments were in accordance with the Directive 2010/63/EU of the European Parliament on the protection of animals used for scientific purposes[9] and were approved by the Internal Evaluation Committee for Animal Welfare in Research of the European Synchrotron Radiation Facility (Grenoble, France). The experiments were performed on 8 male New Zealand White rabbits (2.9 ± 0.1 kg). Anesthesia was induced by IV injection of thiopental sodium (25 mg/kg) via a catheter (22 G) introduced into the marginal ear vein under local anesthesia (5% topical lidocaine). The animal was tracheotomised with a no. 3, Portex tube (Smiths medical, Kent, United Kingdom), and was mechanically ventilated by a commercial neonatal ventilator (Servo-I, Maquet Critical Care, Solna Sweden) with an electronic modification that allowed synchronizing mechanical ventilation with the image acquisition. The initial ventilator settings were adjusted according to the protocol explained further.

The left carotid artery and jugular vein were catheterized for blood gas measurements and for drug delivery. Anesthesia was then maintained with 0.1 mg/kg/h iv midazolam and analgesia was ensured by iv administration of fentanyl (50 µg/kg/h). After ensuring adequate anaesthesia from the hemodynamic parameters, continuous iv infusion of atracurium (1.0 mg/kg/h) was started. The animal was immobilized in the vertical position in a custom-made plastic holder for imaging.

Synchrotron radiation computed tomography imaging

The experiments were performed at the Biomedical Beamline of the European Synchrotron Radiation Facility (ESRF, Grenoble, France). The K-edge subtraction (KES) imaging technique was used as described previously[8 11-13]. This technique allows quantitative measurements of regional specific ventilation ($s\dot{V}$) as well as lung tissue density within the same images. The technique uses 2 X-ray beams tuned at slightly different energies above and below the Xe K-edge (34.56 keV); the binding energy of the K shell electrons. X-rays from a synchrotron radiation source are required since, as opposed to standard X-ray sources, they allow the selection of monochromatic beams from the full X-ray spectrum while conserving enough intensity for imaging with sufficient temporal resolution. Two computed tomography images are thus simultaneously acquired during the inhalation of stable Xe (20 %) in Air. The density due to tissue and to Xe can be separately calculated in each image voxel using a specifically developed computer algorithm [8] explained in detail elsewhere [10]. The "Xe-density" image allows the direct quantitative measurement of this gas within the airspaces, and that of the regional gas volume. Dynamic *KES* imaging during Xe wash-in, or wash-out allows the measurement of regional specific ventilation ($s\dot{V}$)[11]. A "tissue-densit" image obtained from the same data allows the assessment of lung morphology and quantitative measurement of the regional lung aeration [7].

Image analysis

Images were processed by using the MatLab programming package (Mathworks Inc., Natick, MA, USA) as described previously [7]. Lung tissue was selected within the tissue-density computed tomography images, by region-growing segmentation. The local specific ventilation, defined as ventilation normalized to the gas volume within the voxel ($s\dot{V}$), was calculated from the time constant of the Xe wash-in using a single compartment model fit of Xe concentration vs. Time [12]. A 5×5 pixel moving average window was applied to the Xe-density images prior to the model fit. In each $s\dot{V}$ image, the histogram of $s\dot{V}$ was calculated, and fit with a log-normal function. The median (μ) and standard deviation (σ) of the distribution were extracted from the fit. Normal, high and low $s\dot{V}$ was defined with reference to the median value of each slice at baseline. First, the lung tissue density *(D)* in mg/cm^3 was converted to Hounsfield units (HU)[13]. The area of lung comprised within the images was computed and totaled over the 4 axial image slices to calculate the *Total Lung Region of Interest (ROI) Area*. Hyperinflation was defined as a lung density below -900 HU[14]. Lung regions with a density of -900 to 500 Hounsfield units were qualified as normally-aerated (NA), regions with density of -500 to -100 as poorly-aerated (PA), and atelectasis was defined as lung regions with a density from -100 to 0 Hounsfield units, based on previous studies in the literature [14, 15]. In order to characterize the functional behaviour of normally-aerated, poorly-aerated and hyperinflated lung regions, the area of lung within each category was further divided into sub-categories as follows: *no ventilation*, defined as: $s\dot{V} < 0.5$ min^{-1}; *Low* $s\dot{V}$: $0.5\ s^{-1} < s\dot{V} < (\mu - 2\sigma)$; *Normal* $s\dot{V}$: $s\dot{V} = \mu \pm 2\sigma$; *High* $s\dot{V}$: $(\mu + 2\sigma) < s\dot{V}$. Trapping was defined as aerated areas with no $s\dot{V}$. Comparison of lung aeration and $s\dot{V}$ was performed pixel by pixel, and each sub-category was expressed as percentage of the total lung ROI area within the image slice.

Measurement of respiratory mechanics

The airway and respiratory tissue parameters were assessed by using the forced oscillation technique at low frequencies. These measurements were achieved by introducing a loudspeaker-generated small-amplitude (1 cmH_2O peak to peak) pressure forcing signal (0.5-21 Hz) into the trachea via a polyethylene tube (100 cm length, 0.375 cm ID) while the mechanical ventilation was paused at end-expiration. The pressure inside the loudspeaker chamber was maintained at the level of PEEP in order to maintain pressure constant during the recordings. Lateral pressures were measured at the loudspeaker end (P_1) and the tracheal end (P_2) of the wave-tube with miniature pressure transducers (ICS 33NA00D, Malpitas, CA, USA). These pressure signals were low-pass filtered (corner frequency of 25 Hz) and digitized at a sampling rate of 128 Hz. The pressure transfer function (P_1/P_2) was calculated by fast Fourier transformation from the 8-s recordings and the input impedance of the respiratory system (Zrs) was computed from this pressure transfer function as the load impedance of the wave-tube [16]. Three to five Zrs spectra were ensemble-averaged under each experimental condition. A model that includes airway resistance (Raw), inertance (Iaw) in series with constant-phase tissue compartments incorporating tissue damping (G) and elastance (H) was fitted to the averaged Zrs data [17].

Study protocol

At the onset of mechanical ventilation, VC or PRVC ventilation mode was initiated in a randomized order (*Figure S1 in online supplement*). The following settings were used in both ventilation modes: tidal volume: 7 ml/kg; respiratory rate: 40 1/min; PEEP: 3 cmH_2O; inspired oxygen fraction (FiO_2): 0.5. These ventilator settings resulted in an end-tidal CO_2 ($ETCO_2$) of 5.5-6 kPa. After reaching steady-state conditions in systemic hemodynamic and ventilation parameters, a recruitment manoeuvre was performed by inflating the lung to a peak pressure of 30 cmH_2O, in order to standardize the volume history. The animal was then ventilated for 10-min, and a set of Zrs recordings was then collected during short end-expiratory pauses followed by acquisition of 12 subsequent KES images during Xe wash-in at 4 approximately equidistant axial positions from the apical (non-dependent) to the caudal (dependent) lung. The axial positions were standardized based on the apex-diaphragm distance, appreciated on a thoracic projection image. The ventilation mode was then switched and the same measurement sequence was repeated. After the baseline measurements were completed, whole lung lavages were performed by instilling 0.9% saline into the endotracheal cannula at 37º C. Gentle manual suctioning was employed to facilitate lavage fluid withdrawal. The ventilation was resumed for 2 min and this procedure was repeated. A total volume of 100 ml/kg was instilled over 5 sequential lavages. After surfactant depletion, a recruitment manoeuvre was performed as described above, and the respiratory mechanical measurements and the imaging acquisitions were repeated in the same manner as in the baseline condition.

Statistical analysis

The scatters in the parameters were expressed by the SEM values, except for blood gas data where scatter was expressed as interquartile range. The Shapiro-Wilk test was used to test data for normality. Both the mechanical and imaging parameters were normally distributed. Two-way repeated measures ANOVA was applied to evaluate the effects of the variables on the mechanical and imaging parameters with ventilation mode (VC vs. PRVC) and experimental condition (baseline vs. lavage) as within subject variables. Pairwise comparisons were performed by using Holm-Sidak multiple comparison procedures. Pearson correlation tests were performed to test the statistical significance of the relationships between the imaging and respiratory mechanical parameters. The statistical analyses were conducted by SigmaPlot (version 12.5, Systat Software, Inc. Chicago, IL, USA). Statistical tests were carried out with the significance level set at $p<0.05$.

RESULTS

Effect of ventilation modes on airway pressures

The arterial blood gases are summarized in the online data supplement (Table S1). There were no significant differences in the gas exchange indices between the two ventilation modes. Whole-lung lavage deteriorated gas exchange as reflected by a decrease in PaO_2 and an increase in $PaCO_2$ with no detectable alterations in the acid-basis parameters.

The effect of ventilation mode on the ventilation pressures at baseline and following surfactant depletion are shown in Figure 1. Delivering the same tidal volume with the PRVC mode resulted in significantly lower $P_{driving}$ and P_{peak} in the healthy lungs (-13.3±2.7% and -11.1±2.5%, $p<0.001$ for both). Whole lung lavage significantly elevated both $P_{driving}$ and P_{peak} ($p<0.001$) while both of these parameters remained lower with the PRVC mode (-14.0±1.7% and -12.7±1.7% for $P_{driving}$ and P_{peak}, respectively, $p<0.001$ for both).

Effect of ventilation modes on the respiratory mechanics

The airway and respiratory tissue mechanical parameters obtained under VC and PRVC ventilation modes are shown in Figure 2. Surfactant depletion led to a significant deterioration in tissue mechanics independent of the mode of ventilation, with significant increases in G (p=0.02, p=0.03, for VC and PRVC, respectively) and H (p=0.006, p=0.001). These changes were associated with a strong tendency for Raw to increase, which did not reach statistical significance neither under VC (p=0.089) nor PRVC (p=0.054). Overall, there was no evidence for a difference in respiratory mechanics between the two ventilator modes.

Effect of ventilation modes on regional lung function

Figure 2S in the on-line supplement demonstrates sample KES ventilation images, "tissue-density" images showing the distribution of $s\dot{V}$, and maps depicting the regional mechanical behavior of the lung periphery, based on combined aeration and regional ventilation data, in a representative rabbit. Surfactant depletion with whole lung lavage led to the appearance of patchy lung regions with varying degrees of poor aeration, down to complete atelectasis. This heterogeneous deterioration of the regional ventilation resulted in a redistribution of ventilation to the remaining normally-aerated lung regions, which were then unevenly hyperventilated. In contrast with the clearly notable effects of lung lavage, no major difference in regional lung ventilation distribution was apparent between the ventilation modes neither at baseline nor following lavage.

The relative area of lung regions in each of the categories defined based on aeration and s$\dot{V}$ are summarized in Figure 3 and the results of statistical analyses of the corresponding data are summarized in Table 1. Following lavage, the relative area of poorly-aerated lung increased significantly. Part of the poorly-aerated regions had faster specific ventilation, expectedly, due to the reduction in gas volume in these compartments. However, a significant portion of the poorly-aerated regions had either normal or even reduced s$\dot{V}$. The relative amount of atelectatic lung regions significantly increased also. Neither lavage nor ventilation mode had a significant effect on the amount of air trapping. The area of lung regions that were hyperinflated at baseline, was significantly reduced after lavage. Finally, in the remaining normally-aerated lung regions, $s\dot{V}$ was significantly increased in a subset of regions due to ventilation redistribution from non- and poorly-ventilated areas.

Correlation between regional lung function indices and global respiratory mechanics

The relationship between parameters reflecting the area of lung regions in each functional category and the respiratory tissue mechanics are demonstrated on Figure 4. There was a strong and statistically significant correlation between the amount of atelectatic and poorly-aerated lung regions and the magnitude of G and H ($p<0.001$ for both). The correlations between the amount of hyperinflated areas and the tissue mechanical parameters were somewhat weaker, but still statistically significant ($p=0.02$ and $p=0.007$ for G and H, respectively).

DISCUSSION

Detailed analyses of the lung functional differences between the VC and PRVC ventilation modes in the present study highlighted that both modes led to comparable regional lung ventilation distributions, as well as airway and respiratory mechanics. We previously showed that the regional mechanical behavior of the peripheral lung units could be described by combining data on regional aeration and specific ventilation [7]. In the present study, the description of regional lung function using this approach demonstrated no differences between the two ventilation modes in healthy lungs. The similarity in regional lung function between the two ventilation modes were manifested in identical gas exchange parameters with both ventilation strategies in healthy and injured lungs, despite the lower pressures generated by the PRVC mode.

Optimization of mechanical ventilation to provide the best possible gas exchange while maintaining minimal lung inflation pressures is a major challenge in anesthesia an intensive care, particularly in injured lungs. Thus, new ventilation modes have been developed to meet this demand via protective and adaptive strategies to continuous changes in respiratory resistance and compliance. In this regard, PRVC offers the possibility to guarantee the preset tidal volume meeting the gas exchange requirements, with an adaptation of the inspiratory flow to allow the minimization of the positive lung inflation pressure. In agreement with this concept, the results of the present study confirmed the delivery of the guaranteed tidal volume with lower driving and peak airway pressures.

The model adopted in the present study features a highly heterogeneous collapsible lung with the development of poor aeration and atelectasis[18-21], which mimics a key mechanical behavior in ALI [7, 22]. Under this condition, the changes in the respiratory mechanical and regional lung ventilation parameters following lung lavage agreed with those observed previously under similar experimental conditions [7]. The results of the present study allowed not only to evaluate the lavage-induced changes in the indices related to respiratory mechanics and regional ventilation, but also allowed the assessment of the relationships between these outcomes under the two ventilation modes. As far as we are aware, this is the first study to compare airway and tissue mechanical parameters between VC and PRVC ventilation modes.

The most remarkable finding of this study is that despite lower driving and peak airway pressures, the regional ventilation distribution and mechanical behaviour of the lung with PRVC was comparable to that obtained under constant inspiratory flow, in both healthy and injured lungs. The few available studies in the literature comparing the PRVC and VC modes failed to demonstrate the benefit of the former protective approach and even advocated the potential deleterious effects of PRVC[23-25]. However, all of the previous studies used relatively high tidal volumes, generating both high peak inspiratory flows and lung overdistension, which may limit the interpretation of their data in the context of a protective ventilation strategy. Therefore, in line with the recent guidelines on protective ventilation strategy in clinical practice [26], in the present study we targeted a relatively low tidal volume (7ml/kg) with a moderate PEEP of 3 cmH_2O. Under these conditions, there was no evidence of any major adverse effects of PRVC on global lung functional or regional lung ventilation parameters, even in the presence of lung injury promoting alveolar derecruitment (Table 1).

Specific ventilation describes the rate with which Xe washes into the acini in a given lung region. This parameter is therefore determined by both the global minute ventilation, and the local mechanical time-constant of a given lung region. It follows that $s\dot{V}$ is increased by a reduced gas fraction, within the acinar units in an imaged lung region. Conversely, a “normal” or low $s\dot{V}$ in a poorly-aerated region suggests increased resistance of the subtending bronchi, either through narrowing or due to intermittent closure [7, 27]. On the other hand, an increase in $s\dot{V}$ in normally-aerated lung regions implies that these zones receive a larger share of the tidal ventilation. In the presence of highly heterogeneous lung collapse induced by surfactant depletion, functional imaging parameters revealed a significant redistribution of the regional lung ventilation from the poorly aerated areas to zones with normal aeration which had high specific ventilations (Figure 3). Furthermore, a significant portion of the lung, mostly at the boundary of atelectatic regions (Figure 2S), was poorly aerated but showed high specific ventilation. This phenomenon can be interpreted as a reduction in the number of aerated alveoli within these lung units, which show shorter time-constants of xenon washin. Our imaging data showed the development of atelectatic lung regions under both ventilation modes. These phenomena are significant, since they promote mechanical stresses both within non-aerated lung units, and within normally-aerated lung units receiving a larger share of tidal ventilation [7, 28, 29]. The lower driving pressures observed with PRVC imply reduced mechanical stresses despite the redistribution of regional ventilation in a mechanically heterogeneous lung.

The close correlations between oscillatory tissue mechanical and functional imaging parameters suggest that changes in tissue elastance and damping can be a good surrogate for the assessment of the development of altered regional ventilation (Figure 4). The stronger correlations with the amount of atelectatic and poorly-aerated zones suggest that these parameters are more sensitive for detecting lung volume losses. The existence of a negative correlation of G and H with the hyperinflated lung areas, likely reflects the increased elastance within these regions due to an increased surface tension induced by lavage. However, the fact that hyperinflation is positively correlated to elastance in normal lung as shown previously,[7] indicates that the changes in the respiratory tissue parameters can only be clearly evaluated by concomitant measurements of the effective lung volume.[30]

In summary, simultaneous measurements of regional lung aeration and ventilation in a lavage-induced model of ALI provided a quantitative assessment of the changes in regional lung function. Our data show that following whole lung lavage, a significant amount of the lung was poorly aerated yet ventilated. Regional ventilation was redistributed to adjacent regions with normal aeration, a phenomenon which can potentially cause increased stretch in these zones. These phenomena are likely to promote the local concentration of mechanical stresses, and are potentially deleterious to lung tissue. The assessment of the effects of two common mechanical ventilation modes using different inspiratory flow regimes revealed the advantage of applying a decelerating flow ventilation mode (PRVC) to achieve equivalent regional and global lung function in both normal and mechanically heterogeneous lungs, since both the peak and driving respiratory pressures were significantly lower, suggesting a reduced mechanical stress in the lung with a decelerating flow.

Declaration of interests:

Walid Habre has received a research grant from Maquet, Solna, Sweden.

All other authors have no conflicts of interest to declare.

Funding:

This work was supported by the European Regional Development Fund #REG08009 and by the Picardie Regional Council (Amiens, France), the Tampere Tuberculosis Foundation (Helsinki, Finland), the European Synchrotron Radiation Facility (Grenoble, France), Swiss National Science Foundation grant 32003B-143331 (Bern, Switzerland), the Academy of Finland (Helsinki, Finland, grant 126747), Hungarian Basic Scientific Research Grant OTKA K81179 (Budapest, Hungary) and the Department of Anesthesiology Pharmacology and Intensive Care, University Hospitals of Geneva (Geneva, Switzerland).

Author’s contribution:

LP, SB, FP and WH contributed to the conception and design. LP, SB, IM, GA, CD, LB, SS and FP contributed to the experiments, data acquisition, analysis and interpretation. SB, FP and WH drafted the article and all authors revised it critically for important intellectual content and approved the final submitted version. All authors agree to be accountable for all aspects of the work thereby ensuring that questions related to the accuracy or integrity of any part of the work are appropriately investigated and resolved.

Acknowledgements:

This work was performed at the European Synchrotron Radiation Facility (ESRF), Biomedical Beamline-ID17, Grenoble, France. The authors thank Christian Nemoz PhD (ESRF), Thierry Brochard PhD (ESRF) and Herwig Recquart PhD for their technical assistance.

REFERENCES

1 Slutsky AS, Ranieri VM. Ventilator-induced lung injury. *N Engl J Med* 2013; **369**: 2126-36

2 Guldager H, Nielsen SL, Carl P, Soerensen MB. A comparison of volume control and pressure-regulated volume control ventilation in acute respiratory failure. *Crit Care* 1997; **1**: 75-7

3 D'Angio CT, Chess PR, Kovacs SJ, et al. Pressure-regulated volume control ventilation vs synchronized intermittent mandatory ventilation for very low-birth-weight infants: a randomized controlled trial. *Archives of pediatrics & adolescent medicine* 2005; **159**: 868-75

4 Kocis KC, Dekeon MK, Rosen HK, et al. Pressure-regulated volume control vs volume control ventilation in infants after surgery for congenital heart disease. *Pediatric cardiology* 2001; **22**: 233-7

5 Dreyfuss D, Saumon G. Ventilator-induced lung injury: lessons from experimental studies. *American journal of respiratory and critical care medicine* 1998; **157**: 294-323

6 Sjostrand UH, Lichtwarck-Aschoff M, Nielsen JB, et al. Different ventilatory approaches to keep the lung open. *Intensive Care Med* 1995; **21**: 310-8

7 Bayat S, Porra L, Albu G, et al. Effect of positive end-expiratory pressure on regional ventilation distribution during mechanical ventilation after surfactant depletion. *Anesthesiology* 2013; **119**: 89-100

8 Bayat S, Le Duc G, Porra L, et al. Quantitative functional lung imaging with synchrotron radiation using inhaled xenon as contrast agent. *Phys Med Biol* 2001; **46**: 3287-99

9 EU. Directive 2010/63/EU of the European parliament and of the council of 22 September 2010 on the protection of animals used for scientific purposes. *OJ European Union* 2010; **L276**

10 Porra L, Petak F, Strengell S, et al. Acute cigarette smoke inhalation blunts lung responsiveness to methacholine and allergen in rabbit: differentiation of central and peripheral effects. *American journal of physiology Lung cellular and molecular physiology* 2010; **299**: L242-51

11 Bayat S, Strengell S, Porra L, et al. Methacholine and ovalbumin challenges assessed by

forced oscillations and synchrotron lung imaging. *American journal of respiratory and critical care medicine* 2009; **180**: 296-303

12 Porra L, Monfraix S, Berruyer G, et al. Effect of tidal volume on distribution of ventilation assessed by synchrotron radiation CT in rabbit. *J Appl Physiol* 2004; **96**: 1899-908

13 Hounsfield GN. Computed medical imaging. *Science* 1980; **210**: 22-8

14 Vieira SR, Puybasset L, Lu Q, et al. A scanographic assessment of pulmonary morphology in acute lung injury. Significance of the lower inflection point detected on the lung pressure-volume curve. *Am J Respir Crit Care Med* 1999; **159**: 1612-23

15 Gattinoni L, Caironi P, Pelosi P, Goodman LR. What has computed tomography taught us about the acute respiratory distress syndrome? *American journal of respiratory and critical care medicine* 2001; **164**: 1701-11

16 Petak F, Hantos Z, Adamicza A, Asztalos T, Sly PD. Methacholine-induced bronchoconstriction in rats: effects of intravenous vs. aerosol delivery. *Journal of applied physiology* 1997; **82**: 1479-87

17 Hantos Z, Daroczy B, Suki B, Nagy S, Fredberg JJ. Input impedance and peripheral inhomogeneity of dog lungs. *J Appl Physiol* 1992; **72**: 168-78

18 Habre W, Scalfaro P, Schutz N, Stucki P, Petak F. Measuring end-expiratory lung volume and pulmonary mechanics to detect early lung function impairment in rabbits. *Respir Physiol Neurobiol* 2006; **152**: 72-82

19 Bellardine Black CL, Hoffman AM, Tsai LW, et al. Relationship between dynamic respiratory mechanics and disease heterogeneity in sheep lavage injury. *Crit Care Med* 2007; **35**: 870-8

20 David M, Karmrodt J, Bletz C, et al. Analysis of atelectasis, ventilated, and hyperinflated lung during mechanical ventilation by dynamic CT. *Chest* 2005; **128**: 3757-70

21 Rudolph A, Markstaller K, Gast KK, David M, Schreiber WG, Eberle B. Visualization of alveolar recruitment in a porcine model of unilateral lung lavage using 3He-MRI. *Acta Anaesthesiol Scand* 2009; **53**: 1310-6

22 Ware LB, Matthay MA. The acute respiratory distress syndrome. *N Engl J Med* 2000; **342**: 1334-49

23 Roth H, Luecke T, Deventer B, Joachim A, Herrmann P, Quintel M. Pulmonary gas distribution during ventilation with different inspiratory flow patterns in experimental lung injury -- a computed tomography study. *Acta Anaesthesiol Scand* 2004; **48**: 851-61

24 Dembinski R, Henzler D, Bensberg R, Prusse B, Rossaint R, Kuhlen R. Ventilation-perfusion distribution related to different inspiratory flow patterns in experimental lung injury. *Anesth Analg* 2004; **98**: 211-9, table of contents

25 Maeda Y, Fujino Y, Uchiyama A, Matsuura N, Mashimo T, Nishimura M. Effects of peak inspiratory flow on development of ventilator-induced lung injury in rabbits. *Anesthesiology* 2004; **101**: 722-8

26 Dellinger RP, Levy MM, Carlet JM, et al. Surviving Sepsis Campaign: international guidelines for management of severe sepsis and septic shock: 2008. *Crit Care Med* 2008; **36**: 296-327

27 Wellman TJ, Winkler T, Costa EL, et al. Effect of regional lung inflation on ventilation heterogeneity at different length-scales during mechanical ventilation of normal sheep lungs. *Journal of applied physiology* 2012

28 Mead J, Takishima T, Leith D. Stress distribution in lungs: a model of pulmonary elasticity. *J Appl Physiol* 1970; **28**: 596-608

29 Mertens M, Tabuchi A, Meissner S, et al. Alveolar dynamics in acute lung injury: heterogeneous distension rather than cyclic opening and collapse. *Critical care medicine* 2009; **37**: 2604-11

30 Albu G, Wallin M, Hallback M, et al. Comparison of static end-expiratory and effective lung volumes for gas exchange in healthy and surfactant-depleted lungs. *Anesthesiology* 2013; **119**: 101-10

FIGURE LEGENDS

Figure 1: The effect of volume control (VC) and pressure regulated volume control modes (PRVC) on ventilation pressures under baseline conditions (closed symbols) and following lung injury induced by whole-lung lavage (open symbols). *: $p<0.05$ vs. values under VC, #: $p<0.05$ before vs. after lavage-induced lung injury.

Figure 2: Respiratory mechanical parameters obtained under volume control (VC) and pressure regulated volume control modes (PRVC) obtained before (closed symbols) and after (open symbols) lavage-induced lung injury. Raw, G and H: airway resistance, tissue damping and tissue elastance respectively, measured by forced oscillations. #: $p<0.05$ baseline vs. lung injury.

Figure 3. Quantitative distribution of lung regions defined as atelectatic, trapped, poorly-aerated (PA) normally-aerated (NA) or hyperinflated (HI) (mean±SEM). Color scale indicates sub-regions with high, normal or low $s\dot{V}$ within each category; *: $p<0.05$ vs. Baseline, within a condition; **; $p<0.001$ vs. Baseline, within a condition; #: $p<0.05$ vs. VC.

Figure 4: Relationship between the fraction of atelectasis, poor aeration or hyperinflation, expressed as percentages of the total imaged lung area and the respiratory tissue mechanics. G: tissue damping; H: tissue elastance. See text for p-values.

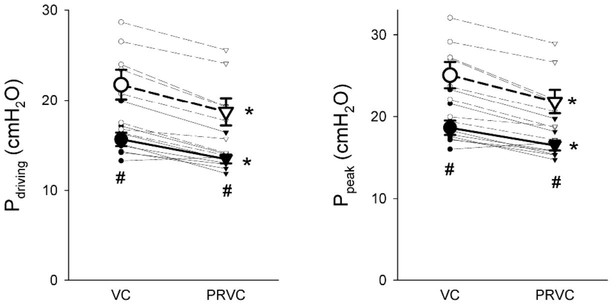

Figure 1

297x420mm (300 x 300 DPI)

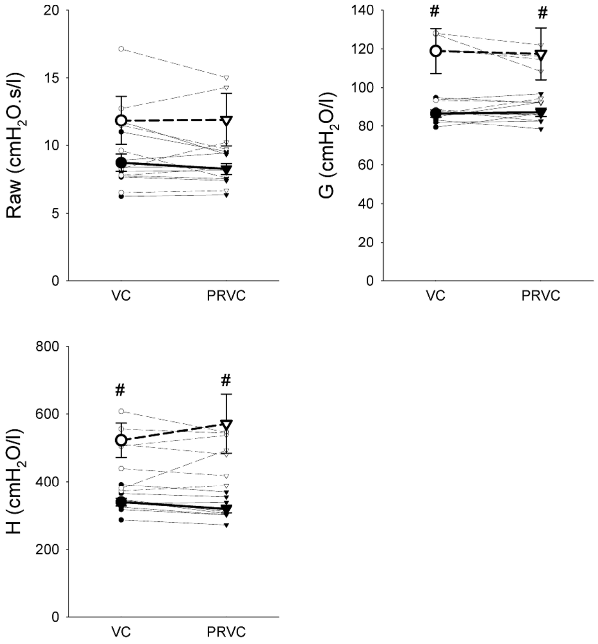

Figure 2

297x420mm (300 x 300 DPI)

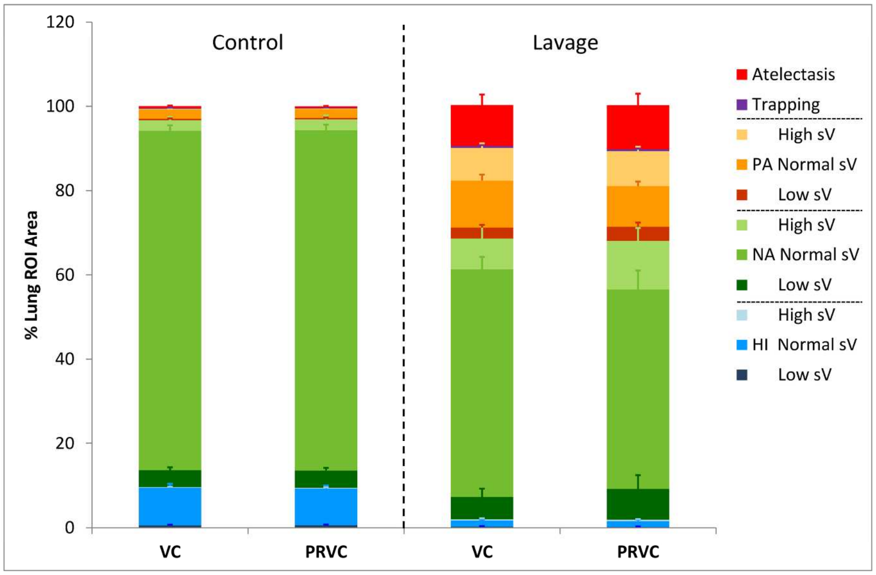

209x148mm (300 x 300 DPI)

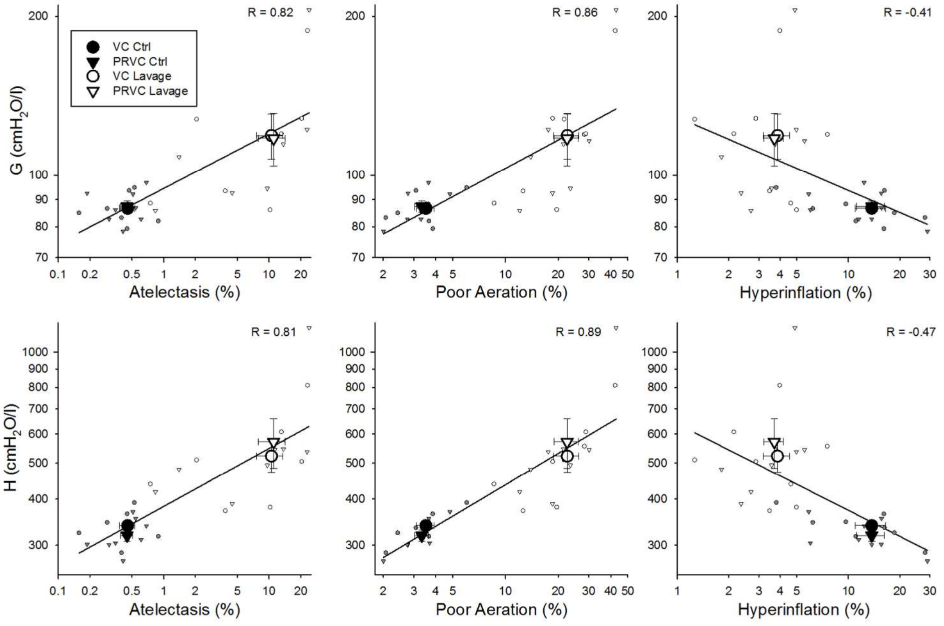

Figure 6

209x147mm (300 x 300 DPI)

Effects of lavage and ventilation modes on regional lung function

		Effect of lavage		Effects of ventilation mode (PRVC vs. VC)	
Aeration	**sV**	**VC**	**PRVC**	**Baseline**	**Lavage**
	Atelectasis	↗	↗	NS	NS
	Trapping	NS	NS	NS	NS
Poor	**High**	↗	↗	NS	NS
	Normal	↗↗	↗↗	NS	NS
	Low	↗	↗	NS	NS
Normal	**High**	NS	↗	NS	NS
	Normal	↙↙	↙↙	NS	NS
	Low	NS	NS	NS	NS
High	**High**	NS	NS	NS	NS
	Normal	↙	↙	NS	NS
	Low	↙	↙	NS	NS

Table 1. Effects of lavage and ventilation modes on the relative areas of lung regions in each of the categories defined based on aeration and s$\dot{V}$. One arrow: $p<0.05$, Two arrows: $p<0.001$.